CHEMISTRY OF MATERIALS
Article

Chem. Mater. **2009,** *21,* 4731–4737 4731
DOI:10.1021/cm9020645

Unique $LaTaO_4$ Polymorph for Multiple Energy Applications

May Nyman,*,† Mark A. Rodriguez,† Lauren E.S. Rohwer,† James E. Martin, Mollie Waller,‡ and Frank E. Osterloh‡

†*Sandia National Laboratories, Albuquerque, New Mexico 87185, and* ‡*University of California, Davis Department of Chemistry Davis, California 95616*

Received July 8, 2009. Revised Manuscript Received August 16, 2009

Rare-earth niobate and tantalate (RE-Nb/Ta) materials are of considerable interest in environmental and energy-related applications that include phosphors for solid-state lighting, photocatalysts for both contaminant degeneration and H_2 generation, chemically robust hosts for nuclear materials and wastes, and ion conductors for lithium batteries or solid-oxide fuel cells. However, the chemically inert nature limits the synthetic routes available to obtain these materials, which in turn hampers the discovery and development of new RE-Nb/Ta phases. Of the simple orthotantalate, $LaTaO_4$, there were three polymorphs known prior. With this paper, we present the structural characterization (from high-resolution X-ray powder diffraction data collected at the APS 11-BM line) of a fourth polymorph. It is obtained only from dehydration of $La_2Ta_2O_7(OH)_2$, which is in turn synthesized hydrothermally. The structure of the new $LaTaO_4$ polymorph is distinctive from the others in the arrangement of the alternating La−O polyhedra layers and TaO_6 octahedra layers. Luminescence measurements (Eu-doped) and photocatalysis studies of the new $LaTaO_4$ polymorph, and comparison to the performance of a previously described $LaTaO_4$ polymorph reveals enhanced performance of the new polymorph in both applications. This study illustrates the relevance of form-function relationships in solid-state materials, as well as the important role of synthesis in the development of advanced functional materials.

Introduction

Doped and undoped rare-earth niobates and tantalates (RE-Nb/Ta) have a unique array of characteristics that include chemical and electrochemical stability, photoelectronic activity,[1−5] ion conductivity[6−9] and luminescence.[10−19] These properties are exploited in a variety of applications that include photocatalysis for H_2 production or photodecomposition of contaminants, solid-state electrolytes, and phosphors. Although the chemical stability of RE-Nb/Ta materials is advantageous for applications, the poor aqueous solubility and high crystallization temperatures hampers expansion and development of the solid-state chemistry of RE-Nb/Ta by limiting opportunity for soft-chemical routes, as well as frustrating solid-state processing. In fact, solid-state processing using temperatures up to 1600 °C and repeated milling of powders is often the protocol to form RE-Nb/Ta powders.[8,20] Thus the discovery of new phases or morphologies (i.e., nanoparticles, thin film coatings) is limited. However, form−function relationships are exceedingly important for tailoring materials for specific applications, both at the atomic scale (composition and crystal structure) and the nanoscale (particle size, surface features, heterostructures). Furthermore, formation of nanoparticles or thin films of these materials by soft chemistry would provide opportunity for utility in devices such as lithium batteries, solid-oxide fuel cells, or light-emitting diodes.

In the interest of expanding the field of RE-Nb/Ta chemistry, both the discovery of new phases[21] and new

*Corresponding author. E-mail: mdnyman@sandia.gov.

(1) Shimizu, K.; Itoh, S.; Hatamachi, T.; Kodama, T.; Sato, M.; Toda, K. *Chem. Mater.* **2005**, *17*, 5161–5166.
(2) Osterloh, F. E. *Chem. Mater.* **2008**, *20*, 35–54.
(3) Abe, R.; Higashi, M.; Zou, Z. G.; Sayama, K.; Abe, Y.; Arakawa, H. *J. Phys. Chem. B* **2004**, *108*, 811–814.
(4) Roof, I. P.; Park, S.; Vogt, T.; Rassolov, V.; Smith, M. D.; Omar, S.; Nino, J.; zurLoye, H. C. *Chem. Mater.* **2008**, *20*, 3327–3335.
(5) Machida, M.; Yabunaka, J.; Kijima, T. *Chem. Mater.* **2000**, *12*, 812–817.
(6) Haugsrud, R.; Norby, T. *Nat. Mater.* **2006**, *5*, 193–196.
(7) Mokkelbost, T.; Andersen, Ø.; Strom, R. A.; Wiik, K.; Grande, T.; Einarsrud, M. *J. Am. Ceram. Soc.* **2007**, *90*, 3395–3400.
(8) Thangadurai, V.; Adams, S.; Weppner, W. *Chem. Mater.* **2004**, *16*, 2998–3006.
(9) vanWullen, L.; Echelmeyer, T.; Meyer, H. W.; Wilmer, D. *Phys. Chem. Chem. Phys.* **2007**, *9*, 3298–3303.
(10) Pang, T.; Cao, W.; Fu, Y.; Luo, X. *Mater. Lett.* **2008**, *62*, 2500–2502.
(11) Blasse, G.; Lammers, M. J. J.; Verhaar, H. C. G. *J. Solid State Chem.* **1985**, *60*, 258–261.
(12) Brixner, L. H.; Chen, H. *J. Electrochem. Soc.* **1983**, *130*, 2435–2443.
(13) Hsiao, Y. J.; Fang, T. H.; Chang, Y. S.; Chang, Y. H.; Liu, C. H.; Ji, L. W.; Jywe, W. Y. *J. Lumin.* **2007**, *126*, 866–870.
(14) Ida, S.; Ogata, C.; Eguchi, M.; Youngblood, W. J.; Mallouk, T. E.; Matsumoto, Y. *J. Am. Chem. Soc.* **2008**, *130*, 7052–7059.
(15) Yan, B.; Xiao, X. *J. Alloys Compd.* **2007**, *433*, 251–255.
(16) Rozhdestvenskii, F. A.; Zuev, M. G. *J. Lumin.* **1983**, *28*, 465–473.
(17) Liu, B.; Han, K.; Liu, X.; Gu, M.; Huang, S.; Ni, C.; Qi, Z.; Zhang, G. *Solid State Commun.* **2007**, *144*, 484–487.
(18) Roof, I. P.; Smith, M. D.; Park, S.; zurLoye, H. C. *J. Am. Chem. Soc.* **2009**, *131*, 4202–4203.
(19) Thomas, M.; Rao, P. P.; Deepa, M.; Chandran, M. R.; Koshy, P. *J. Sol. State Chem.* **2009**, *182*, 203–207.
(20) Haugsrud, R.; Norby, T. *J. Am. Ceram. Soc.* **2007**, *90*, 1116–1121.
(21) Nyman, M.; Rodriguez, M. A.; Alam, T. M.; Anderson, T. M.; Ambrosini, A. *Chem. Mater.* **2009**, *21*, 2201–2208.

Published on Web 09/04/2009

forms such as nanoparticles,[22] we have recently reported a general aqueous route to RE-Nb/Ta materials that has proven very fruitful. From this synthesis, we obtained new structures, $(La,K,\square)_2Nb_2O_{7-x}(OH)_2$ and $Ln_2Ta_2O_7(OH)_2$ ($\square$ = vacancy; Ln = La−Sm).[21] Thermal dehydration of $La_2Ta_2O_7(OH)_2$ results in the crystallization of a new orthotantalate-$LaTaO_4$ polymorph, before converting to a previously reported orthorhombic $LaTaO_4$ ($Cmc2_1$)[23] polymorph at 1200 °C. In this present report, we describe the structural solution from X-ray powder data of the new orthotantalate, referred to herein as **LaTa-850**. In situ heating and X-ray diffraction provided observation of the structural evolution from $La_2Ta_2O_7(OH)_2$ (**LaTa−OH**) to **LaTa-850** to the 1200 °C $LaTaO_4$ polymorph (**LaTa-1200**).[23] Although **LaTa−OH**, **LaTa-1200** and two other previously reported polymorphs of $LaTaO_4$[24−27] all share similar structural features, the structure of **LaTa-850** is notably different.

We also compare here both the luminescence characteristics (Eu-doped) and photocatalytic hydrogen production from methanol of LaTa-850 and LaTa-1200. In both studies, the performances of the two polymorphs are considerably different, providing an excellent example of the intimate relationship between structure and behavior of functional materials. Furthermore, since the unusual LaTa-850 polymorph of $LaTaO_4$ can be only be obtained from dehydration of LaTa−OH; this study also illustrates the importance of synthesis in the process of developing advanced materials.

Experimental Section

Synthesis of LaTa−OH, LaTa-850, and LaTa-1200. $La_2Ta_2O_7(OH)_2$ (LaTa−OH) and Eu^{3+}-doped LaTa−OH were synthesized in a method similar to that which we have reported prior.[21] Briefly, $LaCl_3\cdot 6H_2O$ (0.43 g for 10% Eu-doped, 0.46 g for 5% Eu-doped) and $EuCl_3\cdot 6H_2O$ (0.048 g for 10% Eu-doped, 0.024 g for 5% Eu-doped) are dissolved in 4 mL of DI H_2O. The total amount lanthanum plus europium salt is 1.3 mmol. Potassium citrate (0.42 g, 1.3 mmol) is dissolved in 3 mL of DI water. This solution is added dropwise to the lanthanide salt solution while stirring vigorously, which results in formation of a thick lanthanide citrate precipitate. Thirty drops of 4 M KOH solution is then added, and the precipitate redissolves. The potassium hexatantalate salt[28] (0.42 g) is dissolved in 2 mL DI H_2O and combined with the lanthanide citrate solution in a 24 mL Teflon linear for a Parr reactor. The Parr reactor is placed in a 220 °C oven for 3 days. The white microcrystalline product is collected by vacuum filtration. LaTa-850 is formed by heating dry powder LaTa−OH at 850 °C for 2 h. LaTa-1200 is formed by heating dry powder LaTa−OH at 1200 °C for 2 h.

Table 1. Structural Information, Comparing LaTa-850 to LaTa-1200[a]

	$LaTaO_4$-850	$LaTaO_4$-1200
fw	383.85	383.85
space group	orthorhombic *Pbca* (No. 61)	orthorhombic $Cmc2_1$ (No. 36)
a (Å)	7.8286(1)	3.9313 (9)
b (Å)	11.2180(1)	14.793 (3)
c (Å)	7.4642(1)	5.618 (2)
V (Å^3)	655.52(1)	326.72 (2)
density, calcd (g/cm^3)	7.778	7.803
Z	8	4
R_{Bragg} (%)	7.61	N/A
χ^2	0.81	N/A
R_p (%)	7.1	N/A
R_{wp} (%)	9.4	N/A

[a] From Slobodyanik et al.[23]

Crystallographic Studies of LaTa-850. High-resolution X-ray powder diffraction data were collected at beamline 11-BM located at the Advanced Photon Source (APS).[29] Powders were loaded into mylar capillaries and spun during data collection to improve randomization of the powder pattern. Scan parameters were 2−40° 2θ range with a step-size of 0.005°. Data collection required one hour per pattern. The wavelength used for data collection was 0.45873 Å. Structure solution was performed using the program FOX (version 1.7.5.1),[30] which yielded the La site as well as the location of the Ta−O octahedra. Structure refinement was then executed using GSAS[31,32] where difference-Fourier analysis was employed to locate missing oxygen atoms that were not found in the initial structure solution. The final structure was checked for chemical reasonableness, bond length consistency, and charge balance. The atomic displacement parameters (B_{iso}) were individually refined for the La and Ta cations. In the case of the O atoms, the individual B_{iso} values showed considerable variability. In particular, the O3 site showed unusually low values ($B_{iso} > 0.4$ Å^2), whereas the other O atoms showed B_{iso} values comparable to those obtained for the cations. In addition, significant correlation was observed between the O site positions (xyz) and B_{iso} variables. In an attempt to quell these deviations and thus obtain a more realistic structural model, the B_{iso} values for the O atoms were constrained to be equivalent. This resulted in a lower than expected overall B_{iso} for the O atoms (~0.9 Å^2) that can be traced back to the O3 atom instability during refinement. This anomaly is a shortcoming of the proposed structure model. Table 1 gives the structural information for LaTa-850, as well as that of LaTa-1200[23] for sake of comparison. We attribute the low χ^2 value to the high data to parameter ratio. The atomic positions and thermal parameters are summarized in Table 2. The observed, calculated, and difference spectra for LaTa-850 are shown in Figure 1.

High-temperature XRD analysis was performed using a Scintag PAD X system equipped with a Buehler HDK 1.6 hot-stage. The diffractometer employed a sealed tube X-ray source (Cu Kα) and a peltier-cooled solid-state Ge detector. Diffraction patterns were collected in steps of 50 °C from room

(22) Nyman, M.; Rohwer, L. E. S.; Martin, J. E.; Provencio, P. P.; Rodriguez, M. J. Am. Chem. Soc. **2009**, *131*, 11652–11653.
(23) Slobodyanik, M. S.; Kapshuk, A. O.; Belyavina, N. M.; Markiv, V. Y.; Sich, A. M.; Titov, Y. O. *Dopov. Nats. Akad. Nauk Ukr.* **2003**, 140–145.
(24) Cava, R. J.; Roth, R. S. *J. Solid State Chem.* **1981**, *36*, 139–147.
(25) Kurova, T. A.; Aleksandrov, V. B. *Dokl. Akad. Nauk SSSR* **1971**, *201*, 1095–1098.
(26) Hartenbach, I.; Lissner, F.; Nikelski, T.; Meier, S. F.; Muller-Bunz, H.; Schleid, T. *Z. Anorg. Allg. Chem.* **2005**, *631*, 2377–2382.
(27) Vullum, F.; Nitsche, F.; Selbach, S. M.; Grande, T. *J. Sol. State Chem.* **2008**, *181*, 2580–2585.
(28) Anderson, T. M.; Rodriguez, M. A.; Bonhomme, F.; Bixler, J.; Alam, T. M.; Nyman, M. *Dalton Trans.* **2007**, 4517–4522.
(29) Wang, J.; Toby, B. H.; Lee, P. L.; Ribaud, L.; Antao, S. M.; Kurtz, C.; Ramanathan, M.; Dreele, R. B. V.; Beno, M. A. *Rev. Sci. Instrum.* **2008**, *79*, 085105.
(30) Favre-Nicolin, V.; Cerny, R. *J. Appl. Cyrst.* **2002**, *35*, 734–743.
(31) Toby, B. H. *J. Appl. Crystallogr.* **2001**, *34*, 210–221.
(32) Larson, A. C.; Dreele, R. B. V. *General Structure Analysis System* (*GSAS*); Report LAUR 86−748; Los Alamos National Laboratory: Los Alamos, NM, 2000.

Table 2. Atomic Parameters for LaTa-850

site	multiplicity	x	y	z	B_{iso} (Å^2)
La1	8	0.8660 (3)	0.02413 (7)	0.7433 (3)	2.9 (1)
Ta1	8	0.6242 (4)	0.24212 (9)	0.4976 (3)	2.13 (1)
O1	8	0.651 (2)	0.3092 (6)	0.761 (3)	0.95 (1)
O2	8	0.634 (3)	0.4121 (9)	0.464 (2)	0.95 (1)
O3	8	0.873 (5)	0.262 (1)	0.479 (2)	0.95 (1)
O4	8	0.388 (3)	0.5658 (9)	0.905 (1)	0.95 (1)

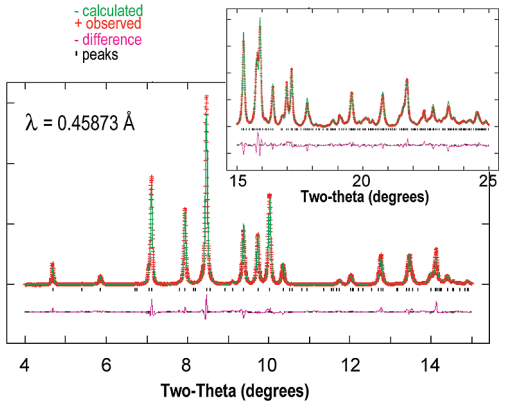

Figure 1. Powder X-ray diffraction data of LaTa-850: observed, calculated, and difference spectra, and peak positions.

temperature up to 1200 °C. Scans parameters were 10−50° 2θ, 0.04° step-size, and 1 s count-time. Each scan required ~16 min. All runs were done in air atmosphere. LaTa−OH powder was placed on top of an alumina substrate, which was placed on the Pt/Rh heating strip. The surface temperature was calibrated on the basis of the thermal expansion values of alumina, accurate to ±5 °C.

Photoluminescence Studies of LaTa:Eu-850 and LaTa:Eu-1200. The photoluminescence (PL) emission and excitation spectra were collected using a Horiba Jobin-Yvon Fluorolog-3 double-grating/double-grating Fluorescence Spectrophotometer. Powder measurements were made by orienting the sample 11° from the incident beam and detecting the emitted light from the front face of the sample. The excitation spectra were collected over the wavelength range of 250−500 nm, with the emission monitored at 614 nm. A complete instrumental correction was performed on all spectra, including corrections for the wavelength-dependent PMT response and grating efficiencies, among other factors. Absolute quantum yield measurements were made by exciting the samples with diffuse light inside an integrating sphere, as described previously.[33]

Measurements of the photoluminescence lifetimes were made under pulsed and DC excitation. For pulsed excitation in the UV (337 nm), a nitrogen laser (PTI GL3300) with a 600 ps pulse width was used. A Thorlabs PDA210 silicon photodiode detector was used to trigger the scope, and a Thorlabs PDA55 silicon photodiode detector was used to measure the luminescence. The luminescence signal was averaged using a 1 GHz Tektronix TDS5104 digital oscilloscope. DC excitation was accomplished with a blue LED emitting at 465 nm, driven by a 50 MHz HP8116 waveform generator. The excitation pulses were long enough to achieve steady-state emission. The Thorlabs PDA55 detector was used to measure the luminescence. The 465 nm LED was found to have an extremely long, low-amplitude emission tail that extends into the red, apparently because of sub bandgap defect states. To block this light from passing through the orange emission filter we placed a blue notch filter in front of the LED.

Diffuse Reflectance. Diffuse reflectance measurements were conducted with an Ocean Optics OOIBase32 UV−vis spectrometer on powdered samples spread on Polytetrafluoroethylene (PTFE) tape. Spectra were calibrated against PTFE tape. The onset of absorption was determined graphically from the intercept of a linear fit of the absorption edge with the abscissa.

Hydrogen-Generation Studies of LaTa-850 and LaTa-1200. H_2PtCl_6 (99.90%, 38−40% Pt) was obtained from Acros Organics and methanol (≥99.8%) was obtained from Sigma-Aldrich. Water was purified to a resistivity of > 18 MΩ cm by a Nanopure II system. Photodeposition of Pt nanoparticles was carried out using a method described previously.[34] A 100 mg sample of LaTa-850 or LaTa-1200 was dispersed in 50 mL of 20 vol % methanol in water also containing dissolved H_2PtCl_6 to yield Pt cocatalyst equal to 1.5 wt % of the $LaTaO_4$ polymorph. The suspension was irradiated with a 300 W Xe arc lamp for one hour with stirring under an Ar atmosphere (approximately 600 Torr). Platinated material was washed four times with 50 mL of water via centrifugation and stored in water for further use. For photocatalytic measurements, a 100 mg sample of platinated lanthanum tantalate was dispersed in 50 mL of water or 20 vol % methanol in water in a quartz flask connected to a gas chromatograph via a valve system. The solution was evacuated and purged three times with Ar gas. The stirred suspension was then irradiated with a 300 W Xe arc lamp for up to five hours. The gas space above the reaction mixture was then analyzed with the GC every hour. Quantum efficiencies were calculated from the generated amounts of H_2 and the quantum flux (5.01×10^{-6} mol/s) for the Xe lamp. The latter was determined by ferrioxalate actinometry.

Results and Discussion

Structure of $LaTaO_4$-850 (LaTa-850), and Comparison to $LaTaO_4$-1200 (LaTa1200) and $La_2Ta_2O_7(OH)_2$ (LaTa−OH). Table 3 compares the Ta−O and La−O bond lengths in LaTa-850 and LaTa-1200, and Table 4 give the bond valence sum values for LaTa-850 and LaTa-1200. Both feature irregular, distorted TaO_6 octahedra with Ta−O bonds ranging from ~1.9 to 2.2 Å and irregular 8-coordinate or 9-coordinate La−O polyhedra with La−O bond distances ranging from ~2.3−3.0 Å.

In comparing LaTa−OH, LaTa-850 and LaTa-1200, we note that the structure of $La_2Ta_2O_7(OH)_2$[21] and $LaTaO_4$-1200[23] most closely resemble each other (Figure 2). This is intriguing, because the evolution of phases by solid-state heating of LaTa−OH is

$$La_2Ta_2O_7(OH)_2 \rightarrow (600\ ^\circ C;\ -H_2O) \rightarrow LaTaO_4\text{-}850\ ^\circ C \rightarrow (1100^\circ C) \rightarrow LaTaO_4\text{-}1200\ ^\circ C \quad (1)$$

The main structural feature of both LaTa−OH and LaTa-1200 is corrugated layers of TaO_6 octahedra, alternating with corrugated layers of lanthanum−oxygen polyhedra (8−9-coordinate La). The origin of the corrugation can be seen most readily in the layers of TaO_6

(33) Rohwer, L. S.; Martin, J. E. *J. Lumin.* **2005**, *115*, 77–90.

(34) Ebina, Y.; Sasaki, T.; Harada, M.; Watanabe, M. *Chem. Mater.* **2002**, *14*, 4390.

Table 3. Comparing Relevant Bond Distances (Å) and Angles (deg) for LaTa-850 to LaTa-1200[a]

atom1	atom2	atom3	$LaTaO_4$-850	atom2	atom3	$LaTaO_4$-1200
La1	O4		2.32 (2)	O2		2.30 (2)
	O4		2.33 (2)	O2		2.30 (2)
	O1		2.42 (1)	O1		2.43 (6)
	O2		2.44 (1)	O1		2.44 (3)
	O2		2.56 (2)	O1		2.44 (3)
	O2		2.70 (2)	O4		2.61 (4)
	O4		2.82 (1)	O2		2.88 (6)
	O3		2.98 (1)	O3		2.94 (4)
				O3		2.94 (4)
	La1		3.916 (3)	La1		3.931 (3)
	La1		4.186 (3)	La1		4.168 (2)
	La1		4.229 (3)			
	La1		4.402 (3)			
	Ta1		3.540 (2)	Ta1		3.487 (3)
	Ta1		3.595 (3)	Ta1		3.625 (2)
	Ta1		3.657 (2)	Ta1		3.815 (4)
	Ta1		3.716 (3)	Ta1		4.264 (2)
	Ta1		3.750 (3)			
	Ta1		3.768 (3)			
Ta1	O1		1.87 (2)	O3		1.94 (5)
	O2		1.93 (1)	O4		1.99 (3)
	O3		1.97 (4)	O4		1.99 (3)
	O3		1.98 (4)	O1		2.03 (6)
	O4		2.11 (1)	O3		2.06 (4)
	O1		2.12 (2)	O2		2.20 (5)
	Ta1		3.736 (3)	Ta1		3.780 (2)
	Ta1		3.918 (4)	Ta1		3.981 (2)
	O1	Ta1	139 (1)	O4	Ta1	142 (2)
	O3	Ta1	168 (2)	O3	Ta1	162 (2)

[a] From Slobodyanik et al.[23]

octahedra, as illustrated in figure 2. Both equatorial and axial oxygen ligands of the distorted octahedra bridge the Ta^{5+} cations: 4 equatorial plus 1 axial for LaTa−OH, and 3 equatorial plus 2 axial for LaTa-1200. On the other hand, the TaO_6 octahedra in LaTa-850 are linked only by Ta−O−Ta equatorial bonds (each TaO_6 linked by all 4 equatorial oxygens), resulting in TaO_6 layers that are not corrugated. The conversion of LaTa−OH to LaTa-850 occurs via loss of a water molecule per formula unit, where the hydroxyl ligands of LaTa−OH are bonded to lanthanum only. Likewise, the coordination of La goes from nine to eight, in the dehydration/conversion of LaTa−OH to LaTa-850; and the La polyhedra go from face-sharing and edge-sharing to just edge-sharing. It is these changes that probably control the "flattening" of the La−O and Ta−O layers in LaTa-850. In LaTa-1200, the La polyhedra return to 9-coordinate La with both face-sharing and edge-sharing, suggesting this more compact type of connectivity is more stable, and the LaTa-850 phase can be considered a metastable intermediate. Both the La−O polyhedra and TaO_6 octahedra for LaTa−OH, LaTa-850, and LaTa-1200 are compared in Figure 2, emphasizing the corrugated layers of LaTa−OH and LaTa-1200 and the relatively flat layers of LaTa-850.

High-temperature X-ray diffraction was used to follow the evolution from LaTa−OH to LaTa-850 to LaTa-1200, shown in Figure 3. This color contour plot shows intensity distribution where the lighter colors indicate strong intensity and darker colors show low intensity. The lower temperature range (25−600 °C) shows peaks that all index to the LaTa−OH pattern. Between 600 and 750 °C the LaTa-850 phase begins to form at the expense of the LaTa−OH phase. This correlates with the observed weight loss (hydroxyl) via thermogravimetry.[21] By 850 °C the material has completely converted to the intermediate compound. Upon further heating to ~1050 °C, the high-temperature form of $LaTaO_4$ is observed. Once the material reaches ~1150 °C, it has fully converted to the high-temperature form. The (012) peak of the alumina substrate at ~25.5° 2θ is detectable above ~200 °C and shifts to lower 2θ values as the sample continues to heat, due to thermal expansion effects. In contrast, some of the indexed reflections of the LaTa−OH phase show shifts to larger 2θ values (shorter *d*-spacings) as the material is heating. These shifts are notable for the (301)/(110) doublet at ~23.5° 2θ as well as the (310)/(202) doublet at ~29.8° 2θ. The peak shifting to smaller *d*-spacing for the LaTa−OH prior to conversion to the LaTa-850 form suggests deformation of the LaTa−OH prior to the phase transition. The nature of this deformation is an area of interest for future studies.

Table 4. Bond Valence Sum (BVS) Calculations for LaTa-850 to LaTa-1200[a]

site	BVS	site	BVS
$LaTaO_4$-850		$LaTaO_4$-1200	
La1	3.34	La1	3.72
Ta1	5.19	Ta1	4.65
O1	2.32	O1	2.29
O2	2.13	O2	2.10
O3	1.90	O3	1.94
O4	2.18	O4	2.03

[a] From Slobodyanik et al.[23]

Photoluminescence. Undoped LaTa-850 and LaTa-1200 exhibit no luminescence under UV excitation. When doped with Eu^{3+} ions, the lanthanum tantalate phases emit narrowband red luminescence. Electronic transitions between the 4f levels of Eu^{3+} produce narrowband emission due to electric and magnetic dipole interactions. The excitation and emission spectra for Eu-doped LaTa-850 and LaTa-1200 are shown in panels a and b in Figure 4. The excitation spectrum of each phase shows several sharp peaks that are attributed to direct transitions within the $4f^6$ configuration of Eu^{3+}. The strongest of these direct excitation peaks is centered at 464 nm, and is much stronger than the peak of the charge transfer band centered at 300 nm. The emission spectrum of LaTa-850 has a strong peak centered at 615 nm, whereas the strongest LaTa-1200 emission peak is at 608 nm. These intense peaks are due to the parity-forbidden electric dipole transition $^5D_0-^7F_2$. This transition is induced by a lack of inversion symmetry at the Eu^{3+} site.

The quantum yield (QY) was found to depend on the crystalline structure. At a Eu^{3+} concentration of 10%, the LaTa-850 phase has a much higher QY (55%) than the LaTa-1200 phase (14.8%) under blue excitation. The QYs for 5 and 10% Eu-doped LaTa-850 and LaTa-1200

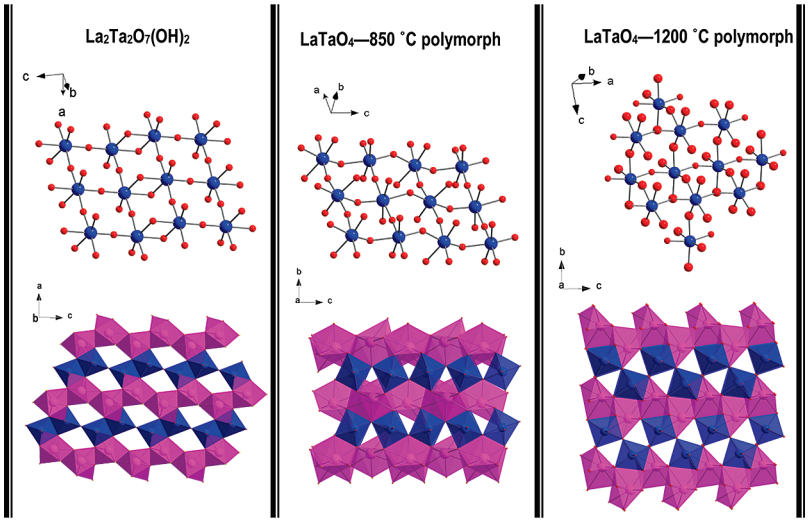

Figure 2. Comparing the layers of LaTa−OH (left),[21] LaTa-850 (middle), and LaTa-1200 (right).[23] Top shows ball-and-stick representations of TaO_6 octahedra (Ta = blue, O = red) connected by both equatorial and axial oxygens in LaTa−OH and LaTa-1200, and by equatorial oxygens only in LaTa-850. This difference in connectivity of TaO_6 octahedra gives rise to corrugated layers for LaTa−OH and LaTa-1200, and relatively flat layers for LaTa-850. This can be seen in the polyhedral representations of the three structures (bottom) where La−O polyhedra are pink and TaO_6 octahedra are blue.

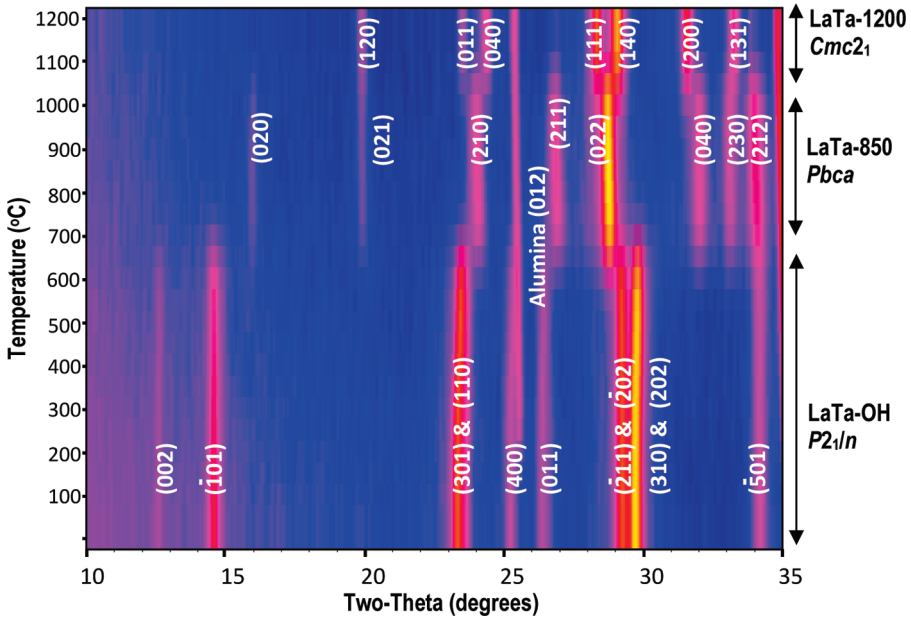

Figure 3. Contour plot of in situ XRD results showing conversion of LaTa−OH to LaTa-850 followed by LaTa-1200. The intensity is a square-route scale; yellow = high counts; blue = low counts (see text for details).

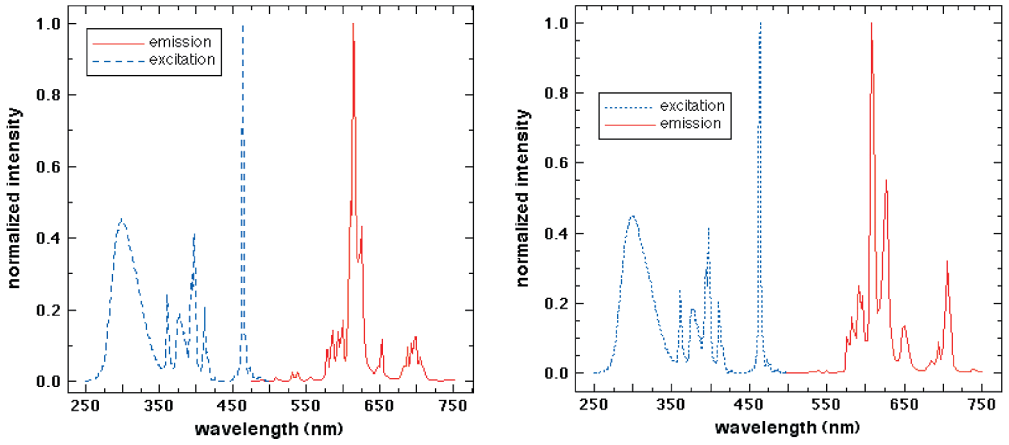

Figure 4. PL excitation and emission spectra for LaTa-850 (left) and LaTa-1200 (right) demonstrating strong direct excitation with blue light.

Table 5. Quantum Yield of $LaTaO_4$:Eu Polymorphs Excited at 464 nm

$LaTaO_4$ polymorph, Eu concentration	QY
LaTa-850, 10%	55
LaTa-850, 5%	51
LaTa-1200, 10%	14.8
LaTa-1200, 5%	6.8

are listed in Table 5. An increase in the Eu^{3+} concentration from 5 to 10% increased the QY of the LaTa-1200 phase from 6.8 to 14.8%. The QY of the LaTa-850 phase does not depend as strongly on the Eu^{3+} concentration. The higher QY for the Eu-doped LaTa-850 is likely due to a lower symmetry of the Eu^{3+} site in the La polyhedra, which results in an enhancement of the $^5D_0-^7F_2$ emission. The La−O polyhedron of the LaTa-1200 polymorph has a mirror plane, whereas as the La−O polyhedron of the LaTa-850 polymorph has no symmetry operations. In the 5 and 10% Eu-doped samples, the structure does not change and change in the unit-cell dimensions is negligible, because of the low concentration. A further increase in the europium-doping of LaTa−OH (15% for instance), following by heating results in crystallization of a mixture of $LaTaO_4$ polymorphs at 800 °C, perhaps including LaTa-850; and neither LaTa-850 nor LaTa-1200 is observed up to 1200 °C. This change in phase may involve the inclusion of K^+-dopants, and the QY of this phase is above 70%. Given the superior brightness of this material, it will be a future immediate topic of study.

The lifetime of the Eu^{3+} emission depends on the crystal structure and the excitation wavelength. Under blue excitation, the emission decays exponentially with lifetimes of 630 and 850 μs for LaTa-850 and LaTa-1200, respectively. Under pulsed UV excitation, the decay cannot be fit by an exponential or stretched exponential function. The lifetime was determined by integrating the normalized signal to compute a harmonic average lifetime. The lifetimes for each phase were found to be comparable: 578 μs for LaTa-850 and 539 μs for LaTa-1200.

Photocatalytic Hydrogen Generation. In order to asses the photocatalytic properties of LaTa-850, and LaTa-1200, 1% (mass) platinum nanoparticles were photochemically deposited onto both materials as described previously.[34] Platinated Pt-LaTa-850 is shown in Figure 5, as an example. The platinated phases Pt-LaTa-850 and Pt-LaTa-1200 were then suspended in aqueous methanol solution (20% v:v MeOH) and irradiated with UV/vis light from a 300 W Xe arc lamp. Under these conditions, the LaTa-850 evolved significant quantities of H_2 (39.1 μmol/h, see Figure 6), whereas LaTa-1200 evolved only traces of H_2 (1.73 μmol/h). The greater activity of Pt-LaTa-850 is likely a result of the reduced bandgap of this phase, which allows for greater light absorption.

Diffuse reflectance spectra for the two $LaTaO_4$ polymorphs are shown in Figure 7. For the LaTa-1200 phase, the absorption onset occurs at 280 nm, corresponding to a bandgap of 4.4 eV, which agrees well with measurements

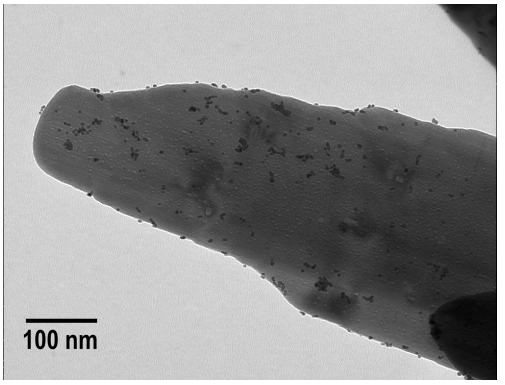

Figure 5. TEM image of LaTa-850 platinized for photocatalysis.

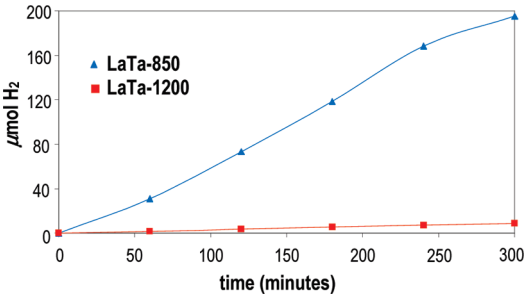

Figure 6. H_2 generation from aqueous methanol solution (20% v/v MeOH), catalyzed by 100 mg of Pt-LaTa-850 and Pt-LaTa-1200 under 300 W Xe-arc lamp irradiation.

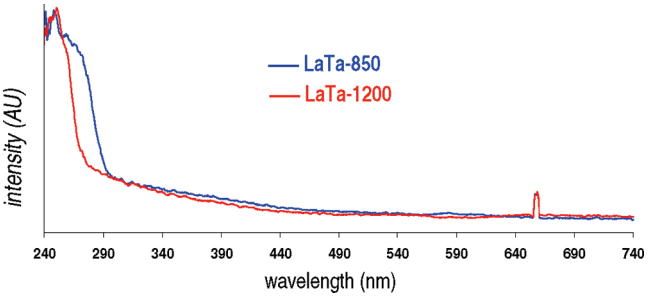

Figure 7. Diffuse reflectance UV/vis spectra for LaTa-850 and LaTa-1200. The artifact at 656 nm is due to the deuterium emission of the tungsten deuterium light source in the spectrometer.

reported by Machida et al.[35] for LaTa-1200. For LaTa-850, the absorption edge occurs at to 300 nm, which translates into a reduced bandgap of 4.1 eV. This bandgap decrease must be of structural origin. The TaO_6 octahedra of the LaTa-850 phase share corners with four other TaO_6 octahedra, with Ta−Ta distances of 2 × 3.736 Å and 2 × 3.918 Å (see Table 3). The LaTa-1200 phase also has each TaO_6 octahedra corner-linked to four other TaO_6 octahedra, and the Ta−Ta distances are 3.780 and 3.931 Å (Table 3). The slightly shorter Ta−Ta distances of the LaTa-850 polymorph may lead to greater electronic interaction among Ta ions, and a lowering of the conduction band edge. The smaller bandgap of LaTa-850 also agrees well with the greater observed photocatalytic

(35) Machida, M.; Murakami, S.; Matsushima, S.; Arai, M. *J. Phys. Chem. B* **2001**, *105*, 3289–3294.

activity of this phase. Finally, both phases also show an absorption tail to about 500 nm that has to be attributed to the presence of Ta^{4+} defect sites.[36]

There have been two recent interesting reports in which the photoluminescence and/or photocatalytic behavior in tantalates and molybdates is correlated with structural parameters. Hu et al.[37] noted the Ta−O−Ta bond angles in undoped $NaTaO_3$ polymorphs are directly correlated with photocatalytic activity and inversely correlated with luminescent intensity. In a different study, Guo et al.[38] observed no luminescence quenching in Eu^{3+}-doped sodium lanthanide molybdates, which was described as being a direct effect of relatively long Ln-Ln distances (~5.0 Å). The Ta−O−Ta bond angles in LaTa-850 and LaTa-1200 are on average nearly identical, 154 and 152°, respectively (Table 3). The La−La distances in LaTa-850 and LaTa-1200 are on average 4.18 and 4.05 Å, respectively. These are considerably shorter than those in the molybdate phase[38] and again very similar for the two lanthanum tantalate polymorphs. The structure−property relationships revealed in these studies on similar phases, however, do not explain the photocatalytic and luminescent behavior we observe in LaTa-850 and LaTa-1200.

Conclusions

In this study, we have presented the synthesis and structural characterization of a new $LaTaO_4$ polymorph, LaTa-850. The synthesis is not conventional; this polymorph can only can be obtained via dehydration of a precursor phase, $La_2Ta_2O_7(OH)_2$, whose synthesis and characterization has also been recently reported. Unlike prior-reported $LaTaO_4$ polymorphs which feature corrugated layers of TaO_6 and La−O polyhedra, LaTa-850 has relatively flat layers, defined by a distinctly different mode of linking the TaO_6 octahedra. We also characterized the luminescence of Eu-doped LaTa-850 and its photocatalytic activity toward H_2 formation from aqueous methanol. In both applications, this new $LaTaO_4$ polymorph exhibited distinctly superior performance characteristics, compared to those of a different $LaTaO_4$ polymorph that is produced by conventional, high-temperature synthesis. This study illustrates the importance of synthesis in the development of functional materials and shows that the behavior of a material can be directly linked to its structure. Ongoing studies include understanding the pathway of conversion of $La_2Ta_2O_7(OH)_2$ to LaTa-850; investigating the structure, composition, and luminescence of lanthanum tantalate with higher Eu concentrations and other codopants; and calorimetric studies of lanthanum tantalate polymorphs.

Acknowledgment. The SNL authors acknowledge Sandia National Laboratories' LDRD program and United States Department of Energy National Energy Technology Laboratory (DE-PS26-06NT42942) for support for this work. F.E. Osterloh thanks the National Science Foundation for supporting this work with an 'Energy for Sustainability Grant' (CBET 0829142). Sandia is a multiprogram laboratory operated by Sandia Corporation, a Lockheed-Martin Company, for the United States Department of Energy under Contract DE-AC04-94AL85000. We thank Lynn Ribaud at APS for his help with specimen preparation, data collection, and file formatting.

Supporting Information Available: Crystallographic information file (CIF) for LaTa-850. This material is available free of charge via the Internet at http://pubs.acs.org.

(36) He, X.; Li, K.; Liu, M.; He, Y.; Zhang, X.; Zhao, Y.; Xue, D. *Opt. Commun.* **2008**, *281*, 2531–2534.
(37) Hu, C.; Tsai, C.; Teng, H. *J. Am. Ceram. Soc.* **2009**, *92*, 460–466.
(38) Guo, C.; Gao, F.; Xu, Y.; Liang, L.; Shi, F. G.; Yan, B. *J. Phys. D.: Appl. Phys.* **2009**, *42*, 1–7.